Absorption Spectra and Optical Constants of Binary and Ternary Solutions of H_2SO_4, HNO_3, and H_2O in the Mid Infrared at Atmospheric Temperatures

U. M. Biermann,*,†,‡ B. P. Luo,† and Th. Peter§

Max-Planck-Institut für Chemie, P. O. Box 3060, D-55020 Mainz, Germany, and Atmospheric Sciences (LAPETH), ETH Zürich, Hönggerberg, CH 8093 Zürich, Switzerland

Received: July 13, 1999; In Final Form: November 9, 1999

Fourier transform infrared transmission (FTIR) measurements of thin films of aqueous sulfuric and nitric acid and their ternary mixture were performed over a wide range of composition and temperature. On the basis of a systematic study of the spectra a database of optical constants for sulfuric acid ($c \leq 80$ wt %) and nitric acid ($c \leq 50$ wt %) for temperatures $183 \leq T \leq 293$ K were obtained. A mixing rule is presented to calculate $k(\bar{\nu})$ and $n(\bar{\nu})$ spectra for $H_2SO_4/HNO_3/H_2O$ solutions and validated against the new FTIR measurements of ternary solutions. This covers optical constants in the entire range of atmospheric relevance and is easily accessible for various applications, e.g., satellite aerosol observations.

I. Introduction

A quantitative evaluation of chemical processes on heterogeneous surfaces in the stratosphere is dependent not only on the chemical and thermodynamic properties of the aerosols (reactivity, solubility), but also on such physical properties as composition, phase, volume and surface area densities. An important source for such information is the collection of different satellite instruments measuring extinction spectra of aerosol particles at widely varying wavelengths. The main constituents of atmospheric aerosols are sulfuric acid (H_2SO_4) and water. In the cold polar stratosphere, a large fraction of HNO_3 can be taken up by the sulfuric aerosol forming a ternary solution. The phase and composition of these binary H_2SO_4/H_2O and ternary $H_2SO_4/HNO_3/H_2O$ particles as well as their number and volume densities may in principle be derived from extinction measurements in the mid infared, e.g., by HALOE (HALogen Occultation Experiment), CLAES (Cryogenic Limb Array Etalon Spectrometer) and ISAMS (Improved Stratospheric And Mesospheric Sounder) onboard the UARS (Upper Atmospheric Research Satellite). However, the interpretation of the observed signal requires additional information, e.g., on the particle size distribution or physical phase, which have to be provided by complementary measurements (e.g., backscatter and depolarization ratios).

Extinction measurements of atmospheric particles in the infrared arise from the absorption and scattering of light at a given wavelength. The interpretation of the measured signal by means of Mie theory requires precise knowledge of the temperature (T) and composition (c) dependent refractive indexes of the main components of the observed aerosol.[1,2] Note that the refractive index $N(\bar{\nu})$ is defined as the sum of the optical constants $n(\bar{\nu})$ (real part of the refractive index) and $k(\bar{\nu})$ (imaginary part of the refractive index). In the mid infrared (2−20 μm), where absorption dominates, the scattering of both acids as well as water reveal pronounced (c,T)-dependent absorption characteristics, requiring detailed knowledge of the optical constants; however, there is only sparse information on the refractive indexes of binary H_2SO_4/H_2O, HNO_3/H_2O, and ternary $H_2SO_4/HNO_3/H_2O$ solutions at stratospheric temperature in the literature. For the H_2SO_4/H_2O system, there are the measurements of Palmer and Williams[3] and Querry et al.[4] for some concentrations at room temperature and additional data for 75 wt % and 96.5 wt % at 250 K.[5] Only recently, new data for binary sulfuric acid at atmospheric temperatures were measured by Tisdale et al.[6] and Niedziela et al.[7,8] For the HNO_3/H_2O system there are some data tabulated by Querry and Tyler[9] as well as some measurements from Boone et al.,[10] but only at room temperature. Optical constants of a ternary solution with 75 wt % H_2SO_4, 10 wt % HNO_3, and 15 wt % H_2O are given by Adams and Downing.[11]

Measurements at lower temperatures are available for solid phases of nitric acid as nitric acid monohydrate (NAM), nitric acid dihydrate (NAD), and nitric acid trihydrate (NAT),[12] as well as glasses of HNO_3 solutions with the stoichiometry $[H_2O]/[HNO_3] = 3$ at 130 K[13] and 140 K.[14]

To approximate the data necessary for the evaluation of atmospheric observations, the optical constants given at room temperature very often are extrapolated to lower temperatures by means of the Lorentz−Lorenz relationship. The physical basis of this rule is the fact that the macroscopic refractivity of a sample can be expressed as the sum of the optical properties of the single molecules contained in the sample.[15] On this basis, the temperature dependence of the refractive index is supposed to be proportional to that of the density of the solutions. There are some examples in the literature where the Lorentz−Lorenz relationship has been successfully used to predict the optical properties of a solution.[5,16,17] However, the applicability of the Lorentz−Lorenz relationship to generate low temperature optical constants for aqueous sulfuric and nitric acid in the mid infrared has to be carefully checked. This is caused by the change of absorption spectra especially of dilute sulfuric acid at low temperatures[7,18,19] due to changes in the degree of dissociation. A change in absorption features directly changes the imaginary part of the refractive index, k, and consequently causes changes in the real part, n, too. For these parts of the spectra the optical

† Max Planck Institute.
‡ Now at Brandenburgisch Technische Universität Cottbus, AG Luftchemie, Max-Planck-Str.11, D-12489 Berlin, Germany.
§ Atmospheric Sciences (LAPETH).

10.1021/jp992349i CCC: $19.00
Published on Web 01/04/2000

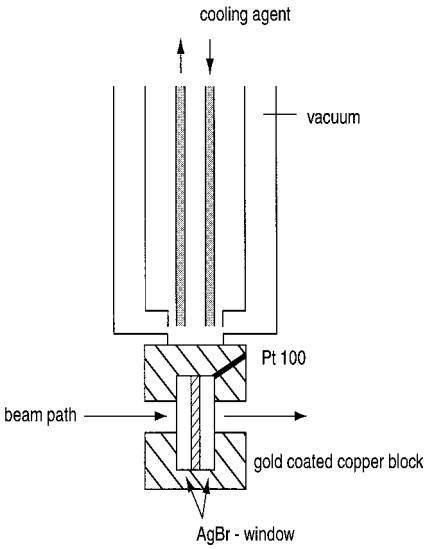

Figure 1. Low-temperature cell for the measurement of liquid acid films and crystalline hydrates.

constants cannot be obtained by extrapolating to lower temperatures using the Lorentz−Lorenz relationship and it is necessary to calculate $k(\nu)$ and $n(\nu)$ on the basis of measured spectra as presented in this work.

Based on a modified Lorentz−Lorenz relationship, Luo et al.[20] showed for wavelengths from the ultraviolet to the near-infrared that the refractive indexes of ternary mixtures of $H_2SO_4/HNO_3/H_2O$ can be calculated using the refractive indexes of the binary aqueous solutions of H_2SO_4 and HNO_3 if an appropriate mixing rule is chosen. The calculation is based on the assumption that the refractivity of a multicomponent mixture can be expressed as the sum of the molar refractivities of the single components if no chemical interaction occurs leading to new species with different optical properties.

In the present work we show that a procedure comparable to the one presented by Luo et al.[20] can describe the optical constants of the ternary solutions in the mid infrared as well. Spectra of ternary mixtures containing sulfuric and nitric acid can be calculated from the binary spectra using an appropriate mixing rule. Comparison with measured spectra of the same composition shows excellent agreement even over a wide range of temperature. A database is assembled and made available on the Internet (see the Conclusions Section).

2. Experimental Setup

We measured the absorption spectra of binary and ternary solutions of sulfuric and nitric acid in the concentration ranges of 10−96 wt % and 10−67 wt % respectively, in the temperature range from 183 to 293 K. For this purpose, a low-temperature cell for transmission spectroscopy of thin liquid films has been developed. The cell is schematically shown in Figure 1. Spectra were taken with a Fourier transform-infrared spectrometer (BOMEM-DA 8). The light beam with wavenumbers 500−5000 cm^{-1} falls on a nitrogen cooled MCT detector after passing the sample, which is sandwiched between two AgBr windows. This material was chosen because it is resistant to the acids and transparent in the wavelength regime of interest. Also, the refractive index of AgBr is low enough to avoid strong interferences at the transitional layers between the strongly parallel windows and the liquid film. The absorption of light can be described by the Lambert−Beer law

$$I(\bar{\nu}) = I_0(\bar{\nu})e^{-\alpha(\bar{\nu})x} \quad (1)$$

where $\bar{\nu}$ is the wavenumber (cm^{-1}), $I(\bar{\nu})$ is the observed intensity of light after passing the sample, $I_0(\bar{\nu})$ is the reference spectrum of the empty cell, $\alpha(\bar{\nu})$ is the extinction coefficient of the absorbing species (cm^{-1}), and x the length of the absorption path. The dimensionless product $(\alpha(\bar{\nu})x)$ is defined as the optical density of the sample; in this study the optical densities are calculated and shown on the basis of the logarithm to the base 10.

Due to the high absorptivity of the acids it was necessary to take spectra of films thinner than ~2 μm to remain in the linear regime of the Lambert−Beer law avoiding saturation effects. A small droplet of the solution was pipetted on one of the AgBr windows (radius $r = 15$ mm) so that a film of about 1−2 μm in thickness formed when the droplet was sandwiched between the two windows. The pair of windows with the film was put into the copper block, which was inserted into the light path of the spectrometer. The spectrometer chamber was evacuated to remove H_2O and CO_2 vapor and to insulate the copper block from room-temperature air.

For calculating the extinction coefficient $\alpha(\bar{\nu})$ from a measured absorption spectrum, knowledge of the exact length of the optical path x, e.g., of the film thickness, is needed. Therefore we initially built up a cell with a fixed distance of the two windows (using a very thin gold foil as the spacer) with the idea of injecting the liquids into the cell producing films of known thicknesses. Unfortunately, because of the very high viscosity of the acids as well as the strong adhesive forces between the acids and the spectroscopic windows, this procedure was not successful. Hence, the film thickness for each sample has to be calibrated using the tabulated optical constants at room temperature given by Palmer and Williams[3] for sulfuric acid and Querry and Tyler[9] for nitric acid as is explained below.

The spectroscopic windows are fixed in the middle of a cold copper block, which is thermostated by a flow of cold ethanol. The temperature is measured by a Pt-100 resistance thermometer in the copper block, close to the optical windows. For calibrating the measured temperature of the liquid we refer to characteristic phase transitons or eutectic temperatures (e.g., the melting point of ice). The transition temperatures are shown in Figure 2. The temperature observed in the copper block is 1 K lower than the actual temperature of the liquids in the cell. The stability of the thermostated temperature is ± 0.1 K.

3 (*T*,*c*)-Dependent Spectra of H_2SO_4/H_2O and HNO_3/H_2O Solutions

Both sulfuric and nitric acid show strongly *c*-dependent absorption features in the mid infrared. In addition, the *T*-dependent dissociation constant of the bisulfate ion causes pronounced changes of absorption features with temperature. Figure 3 shows the *c*-dependent spectra of sulfuric acid in the concentration range from 10 wt % to 96.6 wt % at 293 K, and Figure 4 the *T*-dependence for a 30 wt % solution at three different temperatures. Typical absorption features are the OH stretching region (3200−3500 cm^{-1}), the bending mode of H_2O (1640 cm^{-1}) and the corresponding vibrations of hydrated water ions at 2650−3400 and 1670 cm^{-1}, respectively. The bisulfate ion absorbs at 1341, 1030, 1050, 885, and 593 cm^{-1} and the sulfate ion at 1104 and 613 cm^{-1}. At 1370, 1170, 965, 905, and 564 cm^{-1} the absorption features of molecular H_2SO_4 appear

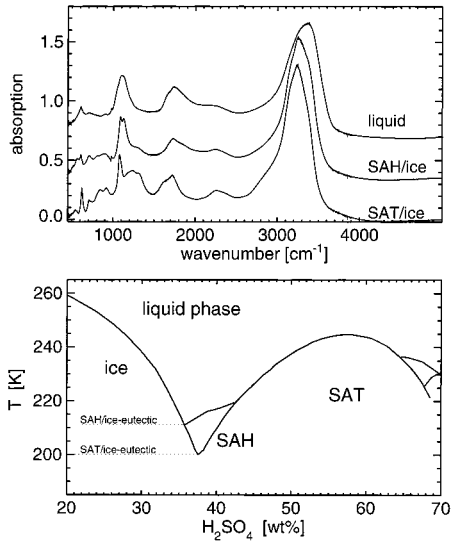

Figure 2. Temperature calibration of the low-temperature cell by means of the phase transition temperatures of a 30 wt % H_2SO_4/H_2O solution. A frozen mixture of SAT ($H_2SO_4 \cdot 4H_2O$) and ice (measured at 198 K) melt above the SAT/ice eutectic temperature. Subsequently a mixture of SAH ($H_2SO_4 \cdot 6.5H_2O$) and ice forms ($T = 199$ K), which melts at the SAH/ice eutectic leaving a 30 wt % solution ($T = 210$ K). A comparison of measured transition temperatures with the tabulated values[21] of SAT/ice (200.1 K) and SAH/ice (211.2 K) shows that the temperature of the probe is 1 K higher than determined by the Pt 100 resistance thermometer. All values are corrected for this offset.

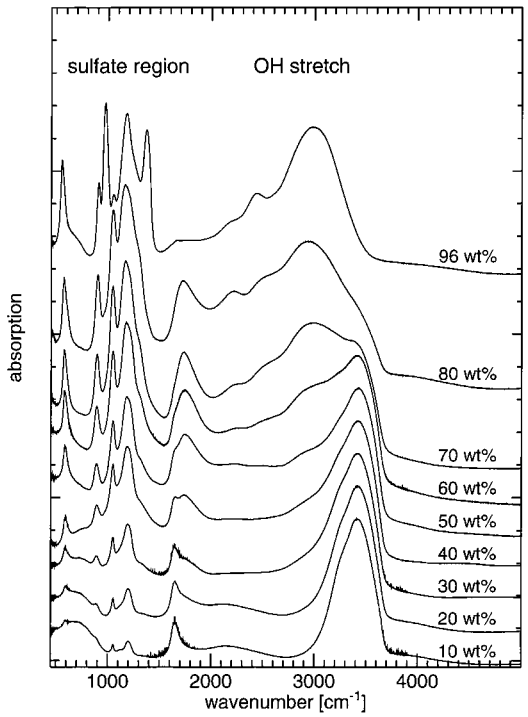

Figure 3. Concentration dependent spectra of binary H_2SO_4/H_2O solutions at room temperature.

in solutions >70 wt %.[22] Figure 5 shows the corresponding spectra of nitric acid in the range from 10 wt % to 65.5 wt % at 293 K and Figure 6 the only weakly *T*-dependent spectra for a 30 wt % HNO_3 solution. While the H_2O and hydrated water ion absorption bands are at about the same wavenumbers, the nitrate ion absorbs at 1350, 820, and 730 cm^{-1}. Absorption features of undissociated HNO_3 molecules[9] are at 2935, 2633, 1672, 1429, 1304, 949, 778, and 691 cm^{-1}. To describe the absorption features in the mid infrared systematically, a matrix

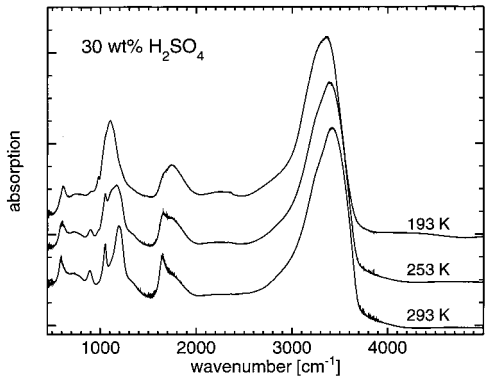

Figure 4. Temperature-dependent spectra of a 30 wt % H_2SO_4/H_2O solution.

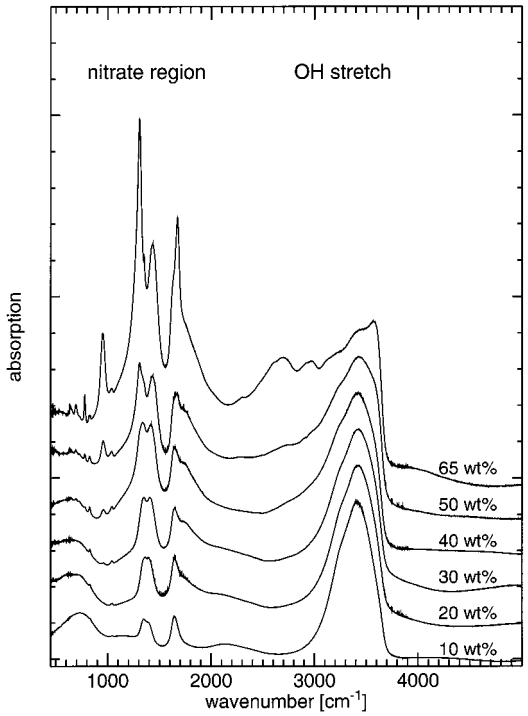

Figure 5. Concentration dependent spectra of binary HNO_3/H_2O solutions at room temperature.

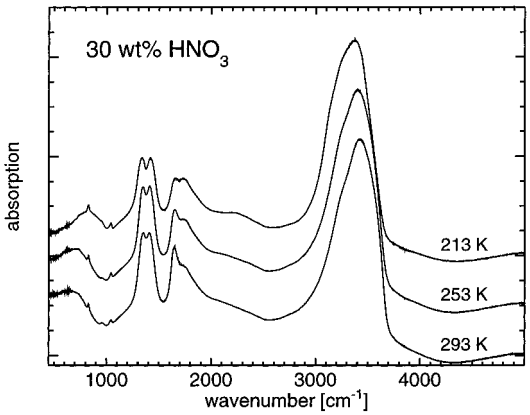

Figure 6. Temperature-dependent spectra of 30 wt % HNO_3/H_2O solution.

of sulfuric acid and nitric acid spectra over a wide temperature and concentration range has been measured (Tables 1 and 2).

The acid spectra reveal that the absorption features of the ionic species change smoothly over a wide range of temperature and composition, as the intensities of the absorption bands are

TABLE 1: List of Measured Binary Sulfuric Acid Spectra[a]

concentration (wt %)	temperature (K)
10	293, 273, 263
20	293, 273, 253
30	293, 273, 253, 233, 213, 203, 193
35	293, 273, 253, 233, 223, 213, 203, 198, 193
40	293, 273, 253, 233, 223
45.6	293, 273, 253, 233, 213, 203
50	293, 273, 253, 233, 223
57.7	293, 273, 253, 233, 213, 203, 193, 188, 183
60	293, 273, 253, 233, 223, 213
64.5	293, 273, 233, 213, 203, 193, 188
70	293, 273, 253, 233, 223
80	293, 273, 233, 213, 203, 193, 188 96.6 293, 273, 243, 233

[a] Temperature and concentration range, where spectra of liquid samples of binary sulfuric acid could be taken; at temperatures below the minimum temperature measured for each sample, the sample crystallized to the corresponding hydrate or ice.

TABLE 2: List of Measured Binary Nitric Acid Spectra[a]

concentration (wt %)	temperature (K)
10	293, 273
20	293, 273, 263
30	293, 273, 253,233, 223
40	293, 273, 253, 233, 213
45	293, 273, 253, 233, 223, 213
50	293, 273, 253, 233, 223
53.8	293, 273, 253, 233, 223 63.7 293, 273, 233, 233, 223

[a] Temperature and concentration range, where spectra of liquid samples of binary nitric acid could be taken; at temperatures below the minimum temperature measured for each sample, the sample crystallized to the corresponding hydrate or ice.

smooth functions of the ionic concentrations in solution. By comparing interpolated spectra with measured ones for some test compositions we reassured ourselves that the entire composition and temperature dependence of the binary H_2SO_4/H_2O and HNO_3/H_2O absorption spectra can be adequately captured by means of a 10 wt %/20 K grid in the regime specified by Tables 1 and 2, and that spectra of other solutions can be accurately derived by linear interpolation. This method covers important features such as the direct dependence of ion concentration on the dissociation equilibrium[7] $HSO_4^- \rightleftharpoons SO_4^{2-} + H^+$. Furthermore, this interpolation method captures finer details such as the red-shift of the OH absorption for lower temperatures, which can be interpreted in terms of a stronger ionization leading to an increase of hydrated H_3O^+ ions at the expense of free water molecules. Because of the comparable water activities in the H_2SO_4 and HNO_3 system, we find comparable OH shifts for both acid systems (see Figures 4 and 6). In summary, because of the smoothly varying absorption spectra with composition and temperature, IR absorption spectra for aqueous binary H_2SO_4 ($\leq$80 wt %) and HNO_3 ($\leq$50 wt %) solutions of arbitrary composition can be calculated by interpolation between solution spectra in the temperature regime specified by Tables 1 and 2.

4. Optical Constants of Binary H_2SO_4/H_2O and HNO_3/H_2O Solutions

Based on the database of absorption spectra obtained by our systematic IR transmission measurements, we now present a method to obtain the optical constants over a wide range of compositions and temperatures.

4.1. Theoretical Background. The refractive index $N(\bar{\nu})$ of absorbing media can be described as a wavelength-dependent complex function

$$N(\bar{\nu}) = n(\bar{\nu}) + ik(\bar{\nu}) \tag{2}$$

where $n(\bar{\nu})$ describes refraction and scattering of light passing the medium, and $k(\bar{\nu})$ describes the absorption. The latter is related to the extinction coefficient $\alpha(\bar{\nu})$ by the relation

$$k(\bar{\nu}) = \frac{\alpha(\bar{\nu})x}{4\pi\bar{\nu}x} = \frac{\alpha(\bar{\nu})}{4\pi\bar{\nu}} \tag{3}$$

The optical density $\alpha(\bar{\nu})x$ is direvtly given by the measured absorption spectrum via eq 1.

The propagation in the x direction of a plane wave with the wave vector κ can be described by

$$E_0^{\,i\kappa x} = E_0 e^{i2\pi\bar{\nu}N(\bar{\nu})x} \tag{4}$$

$$= E_0[\cos(2\pi\bar{\nu}n(\bar{\nu})x) + i\sin(2\pi\bar{\nu}n(\bar{\nu})x)]e^{-[\alpha(\bar{\nu})/2]x} \tag{5}$$

Consequently, the intensity decreases exponentially with the optical density $\alpha(\bar{\nu})x$

$$I = |E_0^{\,i\kappa x}|^2 = E_0^{\,2} e^{-\alpha(\bar{\nu})x} \tag{6}$$

It is important to note that the optical constants $n(\bar{\nu})$ and $k(\bar{\nu})$ are not mutually independent, but fundamentally connected by the Kramers−Kronig relation. By means of this relation the real (imaginary) part of refractive index can be calculated as an integral of the imaginary (real) part for all wavelengths

$$n(\bar{\nu}_0) - 1 = \frac{2}{\pi} P \int_0^\infty \frac{k(\bar{\nu})\bar{\nu}}{\bar{\nu}^2 - \bar{\nu}_0^{\,2}}\, d\bar{\nu} \tag{7}$$

with $n(\bar{\nu}_0)$ equal to the real part of the refractive index at wavenumber $\bar{\nu}_0$, $k(\bar{\nu})$ is equal to the imaginary part of the refractive index at wavenumber $\bar{\nu}_0$, and P the principal part of the integral. Equation 7 can be derived from function theory.[23] There are several different forms of the Kramers−Kronig relation, but the one given by eq 7 is the most practical in the current context.

In the experiments presented here, absorption spectra of the H_2SO_4/H_2O and HNO_3/H_2O system in the range of 500−5000 cm^{-1} were measured. To solve the integral over the whole wavelength regime requires either estimates for those wavelengths not measured or to adapt results from other work covering the undetermined wavelengths. This suggests the separation

$$n(\bar{\nu}_0) - 1 = \underbrace{\frac{2}{\pi} P \int_{0\,cm^{-1}}^{500\,cm^{-1}} \frac{k(\bar{\nu})\bar{\nu}}{\bar{\nu}^2 - \bar{\nu}_0^{\,2}}\, d\bar{\nu}}_{\text{FIR}} + \underbrace{\frac{2}{\pi} P \int_{500\,cm^{-1}}^{5000\,cm^{-1}} \frac{k(\bar{\nu})\bar{\nu}}{\bar{\nu}^2 - \bar{\nu}_0^{\,2}}\, d\bar{\nu}}_{\text{IR}} + \underbrace{\frac{2}{\pi} P \int_{5000\,cm^{-1}}^{50000\,cm^{-1}} \frac{k(\bar{\nu})\bar{\nu}}{\bar{\nu}^2 - \bar{\nu}_0^{\,2}}\, d\bar{\nu}}_{\text{"visible"}} + \underbrace{\frac{2}{\pi} P \int_{50000\,cm^{-1}}^{\infty} \frac{k(\bar{\nu})\bar{\nu}}{\bar{\nu}^2 - \bar{\nu}_0^{\,2}}\, d\bar{\nu}}_{\text{UV}} \tag{8}$$

While absorption spectra $k(\bar{\nu})$ in the mid infrared are directly available from the spectra discussed above and constitute by far the largest term in eq 8, we did not take spectra in the far-infrared ($\bar{\nu} \leq 500\ cm^{-1}$) or at wavenumbers above 5000 cm^{-1}. For the far IR it is reasonable to assume that the absorption

decays monotonically and no significant absorption features occur. Furthermore, there is no contribution of absorption in the visible regime ($\bar{\nu} = 50\,000-5000\ cm^{-1}$) and consequently we set this integral equal to zero. In contrast, the solutions strongly absorb in the ultraviolet ($\bar{\nu} \geq 50\,000\ cm^{-1}$). But as in the integral over the UV region the wavenumber $\bar{\nu}$ is much larger than $\bar{\nu}_0$, this term becomes independent of $\bar{\nu}_0$ and the contribution is a constant.

The absolute value of this constant is determined using the model of Luo et al.,[20] from which the refractive index in the visible (12 820 cm^{-1}, i.e., 0.78 mm) is calculated for the various temperatures and concentrations of interest here. The derived constant is then added to the integral in eq 8.

All calculations of refractive indexes using the database of acid spectra are performed by means of a Fortran routine solving the integral in eq 8. As already mentioned, the validity is limited to $185 \leq T \leq 293$ K and depends on the composition of the solution with total acid concentration up to 80 wt %.

4.2. Measurement Techniques. The calculation of optical constants in this work is based on measured thin film absorption spectra of the acids in the mid infrared. Another technique is to measure the reflectivity at different wavelengths of light falling in normal or near normal incidence on the free surface of a liquid.[3,9] The advantage of the latter technique is that there is no necessity to determine the exact optical path length through the medium, as is necessary in our transmission measurements; on the other hand, during reflectance measurements the strongly hygroscopic sulfuric and nitric acid are in contact with humid air so that changes in composition may occur during cooling. Thus the measurement cell presented here allows simple systematic measurements of various fixed solution spectra at temperatures difficult to assess otherwise, and provides the motivation to determine the thickness of films prepared in our cell. The thickness is required to calculate the wavelength-dependent extinction coefficient $\alpha(\bar{\nu})$ and subsequently $k(\bar{\nu})$ of the solutions.

4.2.1. Calibration of Film Thickness. The film thickness calibration of the measured H_2SO_4/H_2O spectra is performed on the basis of the room-temperature reflectance data given by Palmer and Williams[3] for solutions with 25, 38, 50, 75, and 84.5 wt %, complemented by a measurement of Querry and Tyler[4] at 25 wt %. To derive the film thickness x of individual measurements, we fitted our transmission spectra $\alpha(\bar{\nu})x$ to the $k(\bar{\nu})$ values tabulated by Palmer and Williams[3] (within a factor of $4\pi\bar{\nu}$) over the entire wavelength regime with x being the adjustable parameter (eq 3). The film thickness for the untabulated concentrations were obtained by correlating $\alpha(\bar{\nu})$ (calculated from our calibrated spectra) at the maximum of the OH stretch at ~3400 cm^{-1} with the concentration of the solution given in wt % by mass shown in Figure 7. For concentrations up to 85 wt % we find a linear relationship which we use to determine the extinction coefficient α at this wavelength for any concentration in this range. The linearity of the correlation is plausible given that the absorption strength of the OH stretch is directly related to the water activity of the solutions. The knowledge of the extinction coefficient α at the maximum of the OH stretch vibration subsequently allows us to calculate the thicknesses of all films from the measured optical density.

Figure 8 shows a comparison of the optical constants obtained from our transmission spectra by use of the described calibration procedure and a subsequent Kramers−Kronig analysis and the values tabulated by Palmer and Williams[3] and Querry and Tyler.[4] For the 25 wt % sulfuric acid the agreement of data over the whole wavelength range is better than the error reported for the literature data.

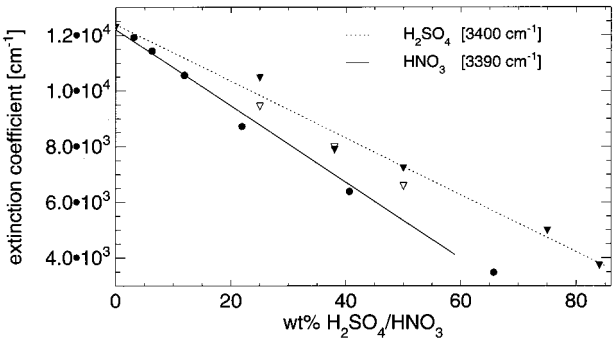

Figure 7. Dependence of extinction coefficient α from the concentration of binary H_2SO_4/H_2O and HNO_3/H_2O solutions at 3400 cm^{-1} (H_2SO_4) and 3390 cm^{-1} (HNO_3). The black triangles represent the values for α obtained from our measured spectra after calibration of film thickness, the open triangles the values reported by Palmer and Williams [1975] at 3400 cm^{-1}. For HNO_3 values of Querry et al. [1980] (black dots) at 3390 cm^{-1} and our values after thickness calibration nearly were identical. The value for pure water (0 wt %) is taken from Wieliczka et al. [1989].

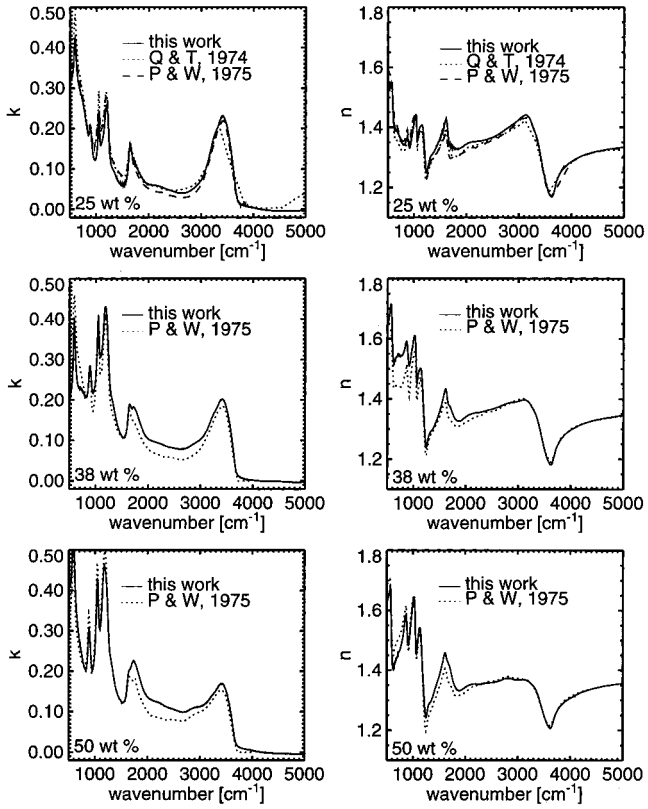

Figure 8. Room tempearure optical constants of binary H_2SO_4/H_2O solutions. A comparison is shown between the values tabulated by Palmer and Williams [1975] (dotted lines) and the values measured in this work (solid lines).

To calculate the film thickness of the measured nitric acid spectra, we fitted our spectra to the values reported by Querry and Tyler[9] for 3, 6, 12, 22, 40, and 65 wt % and used the linear fit of extinction coefficients α of the OH stretch at 3390 cm^{-1} (see Figure 7). A comparison of our data with the spectra given by Querry et al.[9] and Boone et al.[10] is shown in Figure 9.

4.2.1. Temperature Dependence of Optical Constants. As discussed above the absorption spectra of sulfuric acid are T-dependent, thus causing T-dependent $k(\bar{\nu})$ spectra. As all spectra were measured over a wide range of temperatures, it is

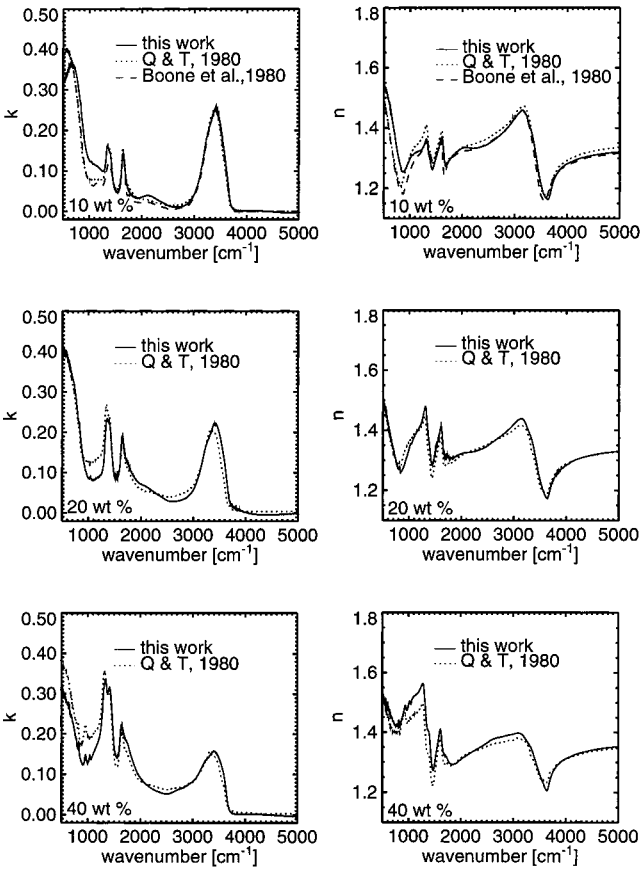

Figure 9. Room-temperature optical constants of nitric acid. A comparison is shown between the values tabulated by Querry and Tyler [1980] Boone et al. [1980], and this work.

possible to calculate the optical constants for all solutions to very low temperatures (as long as they stay liquid, see Table 1). In the following the procedure to calculate optical constants on the basis of the measured spectra will be presented. The temperature-dependent spectra listed in Table 1 were measured by cooling a solution of fixed concentration to low temperatures without changing the film probe. The thicknesses of the films at room temperature were determined as explained in Section 4.2.1. For thin films with high viscosity (e.g., H_2SO_4/H_2O solutions) in the transmission cell the spot on the spectroscopic windows covered by liquid does not change during the cooling process due to the construction of the cell, where the windows with the probe are pressed into a copper block and firmly fixed by screws. Consequently, the change in the thickness of the films is inversely proportional to the density of the liquids. As the *T*-dependent densities of binary sulfuric and nitric acids are well-known,[20] the resulting film thicknesses for the supercooled films can be calculated. Thus the extinction coefficients $\alpha(\bar{\nu})$ and the imaginary part of the refractive index, $k(\bar{\nu})$ are accessible at all temperatures directly from the measured spectra. With the *T*-dependence of refractive indexes in the visible as the boundary condition,[20] it is possible to solve the integral given in eq 8 and thus to determine the real part $n(\bar{\nu})$ of the refractive index in the temperature range from 185 to 300 K. Figure 10 shows the absorption spectrum (optical density), the imaginary part *k* and the real part *n* of the refractive index of a 30 wt % H_2SO_4/H_2O solution at 293 and 203 K. Especially in the sulfate region (900−1250 cm^{-1}) the change with temperature in the absorption spectrum is clearly reflected in the $k(\bar{\nu})$ and $n(\bar{\nu})$ spectra. The greatest change in $k(\bar{\nu})$ for a 30 wt % H_2SO_4/H_2O solution is at $\bar{\nu} = 1100$ cm^{-1}. In this wavelength region *k*

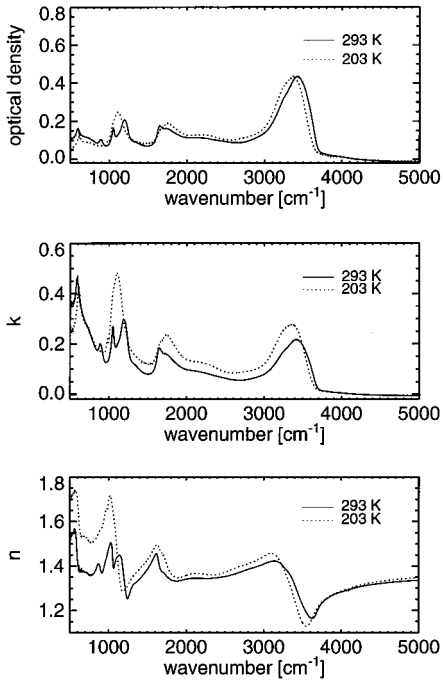

Figure 10. Temperature dependence of optical constants for a 30 wt % H_2SO_4/H_2O solution. The change in absorption features especially in the sulfate region (900−1250 cm^{-1}) leads to significant changes in the *k* and *n* values.

increases from 0.201 to 0.513 (a factor of 2.55) for a temperature change from 293 to 203 K. The real part of the refractive index *n* follows this difference wavelength shifted at 1050 cm^{-1}, changing from 1.505 at 293 K to 1.717 at 203 K (a factor of 1.14). As mentioned above, these changes can be traced back to the dissociation of HSO_4^- ions, see also Niedziela.[7,8]

4.3. Optical Constants of H_2SO_4/H_2O Solutions. The change in absorption spectra of diluted sulfuric acid solutions is based on the *T*-dependent dissociation constant of the sulfate-bisulfate system and consequently appears for all spectra with concentrations ≤50 wt %. Additionally we observe a temperature dependent change in the shape of the OH stretch for all spectra in this concentration range. As the solutions are cooled, the OH band becomes narrower, resulting in a higher maximum value of the extinction coefficient α at ∼3400 cm^{-1}. In parallel the maximum shifts slightly to smaller wavenumbers. Presumably the changing shape and maximum of the OH stretch reflects the increasing effective mass of the vibrating clusters due to H-bridges induced by the sulfate ions. The increase in α (3400 cm^{-1}) with decreasing temperatures and acid concentrations can be empirically described using $\alpha = a + b \cdot wt + (c + d \cdot wt + e \cdot wt^2)/T$, where *wt* is the composition of the solution in percent by mass. Figure 11 shows the extinction coefficients (black dots) for solutions with 10, 20, 30, 40, 45, 50, 57, and 64 wt % computed from the measured spectra assuming that the film thickness is inversely proportional to the density of the solution. Additionally the measured temperature-dependent spectra of pure water at 293, 273, and 263 K, along with the same fit for α (3400 cm^{-1}) is shown in this figure. The parameters of the fit equations are given in the figure caption. The fit in Figure 11 enables us to convert any measured or interpolated absorption spectrum ($c \leq 64$ wt %) to a $k(\bar{\nu})$ spectrum. For higher concentrated solutions the *T*-dependence was adapted from the results of Tisdale et al.,[6] who report optical constants for 75 and 80 wt % at 215 K. We compared their measurements with our room temperature measurements and found only a small

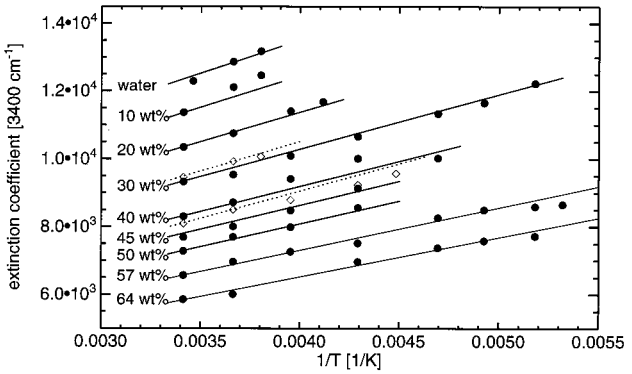

Figure 11. Temperature dependence of extinction coefficient α at the maximum of the OH stretch vibration. The lines represent a fit of the form $\alpha = 5596.0 - 58.33wt + ((1\,980\,000.0 - 11958.0)\cdot wt - 12.43\cdot wt^2)/T$ for H_2SO_4 (solid lines and dots) and $5476.4 - 95.4\cdot wt + ((1\,980\,000.0 - 11\,958.0)\cdot wt - 12.43\cdot wt^2)/T$ for HNO_3 (dashed lines and diamonds).

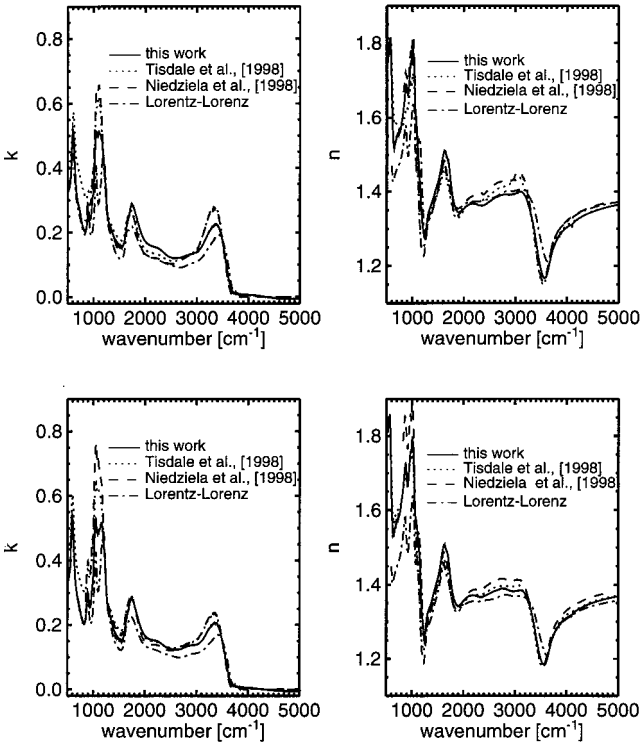

Figure 12. Comparison of optical constants calculated in this work with values given by Tisdale et al. [1998], Niedziela et al. [1998], and optical constants caculated applying the Lorentz−Lorenz relationship (see text). Concentration and temperatures of the compared data sets were chosen as close together as possible. Upper pictures: this work: 45 wt % H_2SO_4, 213 K; *Tisdale*: 45 wt %, 215 K; *Niedziela*: 43 wt %, 220 K. Lower pictures: this work: 50 wt % H_2SO_4, 223 K; *Tisdale*: 50 wt %, 215 K; *Niedziela*: 50 wt %, 220 K.

temperature dependence which is reasonable for the highly concentrated solutions.[5]

The Kramers−Kronig analysis presented above allows the real part of the refractive index to be calculated for these spectra for H_2SO_4/H_2O solutions from 10 to 85 wt % at 193−293 K. To test the validity of this procedure we compare our optical constants with other measurements in the same concentration and temperature range. Recently, Tisdale et al.[6] and Niedziela et al.[7] published optical constants in the mid infrared for aqueous sulfuric acid with concentrations higher than 45 wt % at 215 K. A comparison of the three data sets is shown in Figure 12. There is in general a good agreement in the main special features

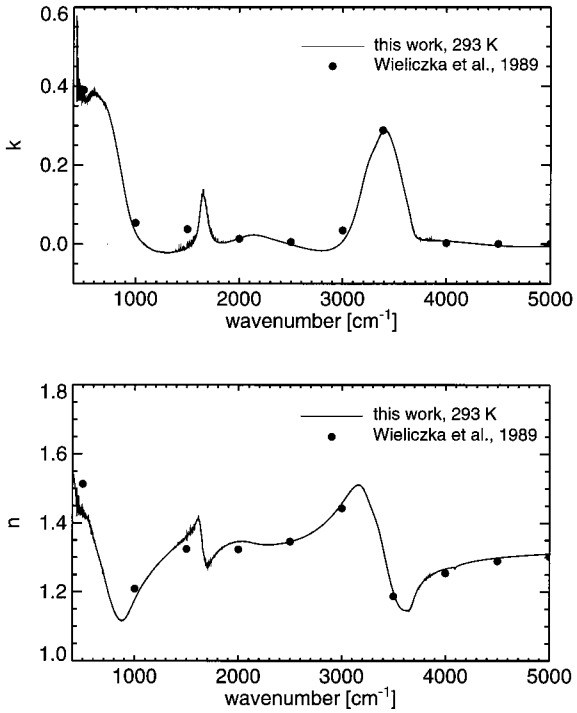

Figure 13. Optical constants of water: the black line represents the *k* and *n* values calculated from our spectra, whereas the black dots show the average of values reported in the literature [Wieliczka et al., 1989].

although it has to be stated that remarkable differences in the imaginary part of the refractive indexes exist, especially in the maximum of the OH stretch vibration as well as in the sulfate peak at ∼1100 cm^{-1}. There is some uncertainty in our data caused by the calibration of film thickness, which had to be performed using tabulated literature data. We minimized the influence of possible errors in the reference data (e.g., caused by saturation of highly absorbing species) by fitting the film thickness over the whole wavelength region. However, it should be clearly noted that uncertainties in film thickness cannot be made responsible for the observed deviations: a variation in film thickness causes a linear change of our $k(\bar{\nu})$ spectra, not increasing or decreasing single absorption peaks and consequently does not help in bringing the three data sets into better agreement. Therefore we believe that the differences between the data sets are reflecting uncorrelated problems of all three methods used. Especially the smooth increase and decrease of the water and sulfate absorption with temperature and concentration reflected in our spectra gives us high confidence in our tabulated data sets. In any case, the unsuitability of the Lorentz−Lorenz relationship to obtain low-temperature optical constants for binary sulfuric acid solutions becomes clearly evident from the comparison of all three measured low-temperature data sets. As can be seen in Figure 12, too, the optical constants obtained by the Lorentz−Lorenz relationship and used to extrapolate from room-temperature data to atmospheric temperatures (dashed-dotted line) clearly underestimates the *T*-dependence of the absorption spectra. Hence, the resulting $k(\bar{\nu})$ and $n(\bar{\nu})$ values are too low.

An additional important test of the validity of the proposed procedure is the comparison with optical constants for water given in the literature. A good survey of optical constants is given by Wieliczka et al.[24] No low-temperature optical constants are reported up to now. Figure 13 shows good agreement of our results with the average of all values reported, which further speaks for the quality of our data.

4.4. Optical Constants of HNO_3/H_2O Solutions. The same procedure as described for sulfuric acid solutions leads us from the measured spectra to the temperature-dependent optical constants for binary nitric acid solutions, too. Temperature-dependent spectra were measured in the concentration range of 10−50 wt % and the temperature range from room temperature to 213 K as long as the solutions stayed liquid (see Table 2).

Based on room-temperature data for HNO_3/H_2O solutions,[9] the temperature dependence of the optical constants was calculated by assuming the change in the thickness of films to be inversely proportional to their density during the cooling process in the transmission cell. Since the viscosity of nitric acid and thus the adhesive forces to the spectroscopic windows are lower than for sulfuric acid, some of the films tore during the cooling process. Nevertheless, when the film remained intact (e.g., 20 wt % HNO_3/H_2O, 30 wt % HNO_3/H_2O), the temperature dependence of α could be well analyzed and the temperature dependence of the extinction coefficient at the OH stretch vibration is comparable to that of sulfuric acid with the same composition in wt % (see Figure 11). While the slope of the fitted line is nearly identical for 20 and 30 wt % HNO_3/H_2O and H_2SO_4/H_2O solutions, the absolute values of α are different. The temperature dependence of the extinction coefficients in the maximum of the OH stretch could be expected as α is correlated with the activities of the solutions as pointed out above. For the further parametrization of the optical constants of nitric acid we use the same fit parameters for the slope of temperature dependence as were used for sulfuric acid with the same composition and adapt them to the absolute values of absorptivity obtained from the calibrated spectra.

These are the first low-temperature optical constants for the HNO_3/H_2O solutions reported in the literature. From Figures 4 and 6 it can be seen that the temperature dependence of the optical constants for this acid is not as pronounced as for sulfuric acid. This is due to the fact that nitric acid only has one dissociation stage and consequently shows only a small change in the absorption spectra when the temperature is reduced.

5. Optical Constants of Ternary $H_2SO_4/HNO_3/H_2O$ Solutions

In section 4 we provided a database of measured binary sulfuric and nitric acid spectra together with an interpolation scheme to derive optical constants of binary HNO_3 and H_2SO_4 solutions over a wide temperature and composition range.

Next, we determine the optical constants of the ternary $H_2SO_4/HNO_3/H_2O$ solutions in an atmospherically relevant composition and temperature range. Luo et al.[20] showed that the refractive index of ternary $H_2SO_4/HNO_3/H_2O$ solutions over a wavelength range from 0.2 to 2 μm can be calculated by using a mixing rule based on the Lorentz−Lorenz relationship. A similar approach is made here for the optical constants of ternary solutions in the mid infrared. We assume that the absorption spectra of ternary solutions can be composed of spectra of the binary solutions

$$\mathrm{Y}(\lambda,T,W_s,W_n) = \frac{W_s}{W_s+W_n}\,\mathrm{Y}_s(\lambda,T,W_s^{\,b}) + \frac{W_n}{W_s+W_n}\,\mathrm{Y}_n(\lambda,T,W_n^{\,b}) \quad (9)$$

where Y is either the absorption spectra (given by $\alpha(\bar{\nu})$) or the optical constant $k(\bar{\nu})$. In eq 9 W_s and W_n are the weight percentages of H_2SO_4 and HNO_3 in the ternary solution and $W_s^{\,b}$ and $W_n^{\,b}$ the weight percentages for spectra of binary sulfuric acid and nitric acid solution (Y_S,Y_N), respectively.

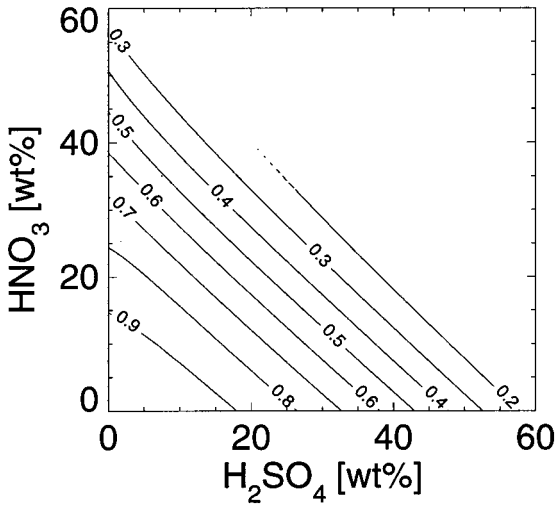

Figure 14. Activities of water for different ternary solutions at 293 K. Note that the activity of water is nearly a constant for solutions with a fixed value of $W_S + W_N$.

This treatment is based on the following arguments. The absorption features of sulfate and nitrate as well as water ions (or molecules) in a ternary solution should be very similar to those in the corresponding binary solution, if the ternary solution has similar ionic strength or a similar water activity, provided that the species do not react with each other and no new substances with additional absorption features occur in the mixture. By means of an ion interaction model (parametrization given in Luo et al.[25]) we have shown earlier that for both binary solutions and their ternary mixtures, the activity of water is very similar in solutions with the same total acid concentration in wt % by mass. The quality of this approximation is checked by means of the ion interaction model in Figure 14. Given the good agreement we choose as a mixing rule

$$W_b^{\,s} = W_b^{\,n} = W_s + W_n \quad (10)$$

for the evaluation of eq 9. For the validation of this mixing rule, in Figures 15 and 16 we compare optical constants of some ternary solutions obtained from ternary spectra measured in our transmission cell with those calculated by using eqs 9 and 10. The good agreement suggests that the calculated optical constants are of similar accuracy as our measured ones. Interestingly, the agreement of the absorption features is nearly perfect. The major differences most likely come from the residuals of a baseline subtraction.

By means of this new mixing rule we are also able to determine the unknown compostion of a ternary solution. By minimizing the square of the deviation between a measured and a calculated spectrum of a given solution with a numeric fitting procedure we can obtain the composition of the ternary solution (see Figure 17). This gives us a method to determine the composition of aerosols, not only under laboratory conditions, but also for atmospheric remote sensing measurements. Other calibration procedures have been much less precise due to overlapping absorption features of sulfate and nitrate ions in the range between 500 and 2000 cm^{-1}.[26] Using our laboratory measurements of ternary solutions we can test the mixing rule given in eqs (9 and 10) by comparing the fitted composition and the true composition of the measured samples. Alternatively, we tested other mixing rules for the linear combination of spectra

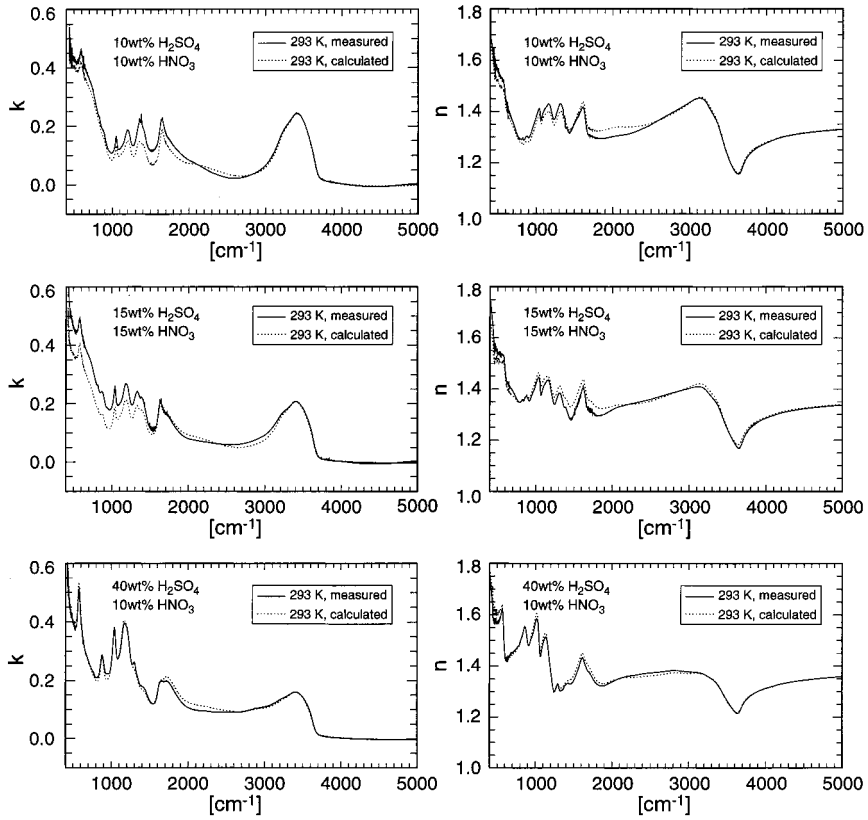

Figure 15. Comparison of optical constants derived from measured spectra (black line) and calculated using eqs 10 and 11 (dotted line) for ternary solutions of three characteristic compositions.

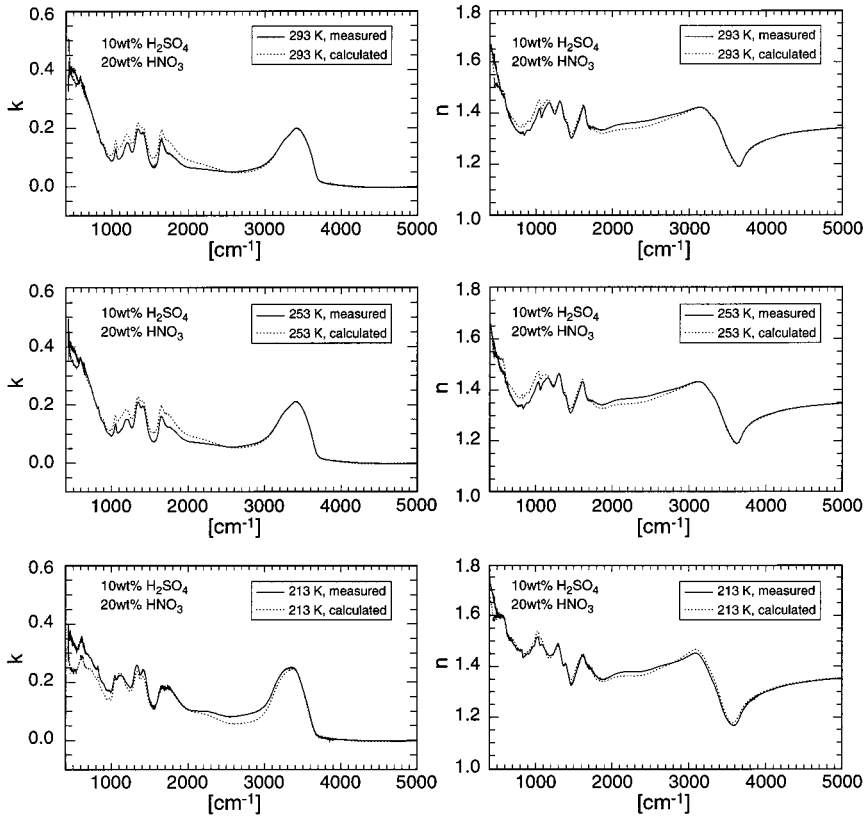

Figure 16. Comparison of optical constants derived from measured spectra (black line) and calculated (dotted line) for a ternary solution containing 10 wt % H_2SO_4 and 20 wt % HNO_3 at three different temperatures.

of ternary solutions using for example molar units (molarity, molality) instead of weight percent W_s^b and W_n^b for the mixing of spectra. Furthermore, we have also used independent W_s^b and W_n^b values (without the constraints of eq 10). In any of these cases the agreement was less satisfactory than when using eq 10.

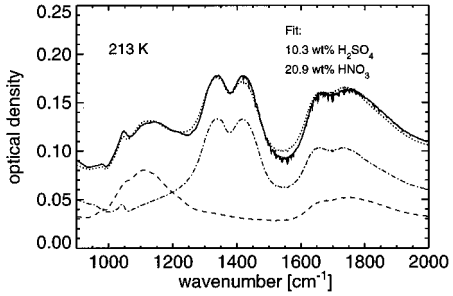

Figure 17. Analysis of composition of a $H_2SO_4/HNO_3/H_2O$ spectrum by means of the database of spectra. To test the fit procedure a solution with 10% H_2SO_4 and 20 wt % HNO_3 was mixed and a spectrum at 213 K was taken. The black line shows the measured spectrum, compared with the calculated fit (dotted line). The dashed line represents the share of a binary H_2SO_4/H_2O solution, the dashed−dotted line that of the binary HNO_3/H_2O solution. The determination of composition is better than 1%.

The concentrations determined from this mixing rule are in good agreement with the actual concentration of the samples (see Figures 17, 18). The agreement between the measured spectra and the fitted spectra is excellent, even at very low temperatures. This corrobates the statement that the absorption features of ions are similar in ternary and binary solutions with comparable ionic strength and water activity.

6. Atmospheric Implications

The knowledge of the optical constants for binary sulfuric and nitric acids and their ternary mixtures in the mid infrared is of vital interest for the interpretation of the observed extinction signal from atmospheric aerosols. Especially the imaginary part of the refractive index, $k(\bar{\nu})$, is important, because in this wavelength region the strong absorption dominates scattering for the species of interest. The strong influence of the absorption pattern on the evaluation of the atmospheric aerosol loading is underlined in Figure 19, where we show the extinction coefficient (km^{-1}) calculated for a particle size distribution of sulfate aerosol at normal background conditions (log-normal distribution with $n = 10$ cm^{-3}, $r_0 = 0.725$ μm, $\sigma = 1.6$) for a 50 wt % solution at 220 K on the basis of the complex refractive index measured in this work. For comparison we plotted the same variable on the basis of optical constants obtained by applying the Lorentz−Lorenz relationship to extrapolate from room-temperature data to 220 K as well as the data sets given by Tisdale et al.[6] and Niedziela et al.[7] It becomes evident that the use of optical constants obtained from the Lorentz−Lorenz relationship for the evaluation of atmospheric observations in the mid infrared may lead at certain wavelengths (e.g., the sulfate region around 1100 cm^{-1}) to an overestimation of the aerosol loading of up to 40%. Note that this is a relevant uncertainty when compared to trends of 5% per year, which have been discussed recently in the context of a potential aircraft-induced increase in lower stratospheric aerosol loading.[27] However, there are also still significant differences between the laboratory data of Tisdale et al.,[6] Niedziela et al.,[7] and the present work. This causes further uncertainties in the interpretation of the observed signal. While the origin of these deviations is unclear at present, the two previously measured data sets show even higher values of absorption in the strongly absorbing OH and sulfate region, which would further increase the discrepancy from the Lorentz−Lorenz results. Clearly, it is necessary to employ low temperature optical constants provided by laboratory measurements, not only for binary sulfuric acid but for nitric acid and their ternary mixtures, if a sensitive evaluation of the mid infrared field observations is the aim. In this respect, the database presented in this work enlarges the available data basis and helps to improve the knowledge on important atmospheric features.

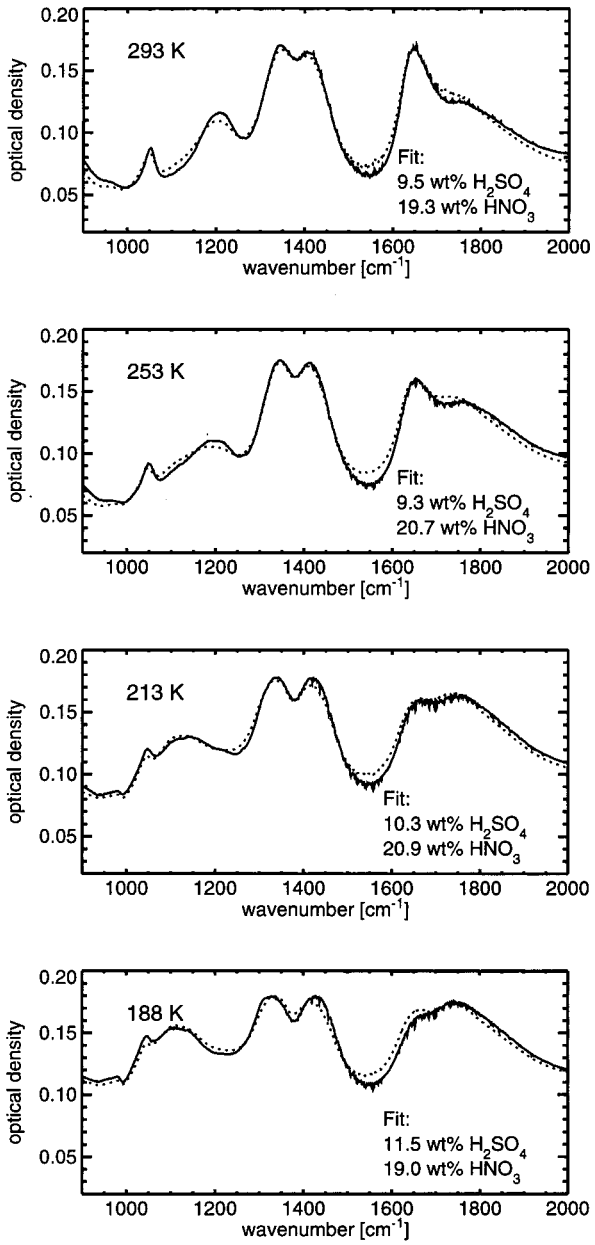

Figure 18. Temperature dependence of composition analysis for ternary solutions. The solution contains 10 wt % H_2SO_4 and 20 wt % HNO_3.

7. Conclusions

A systematic study has been performed of absorption spectra of aqueous sulfuric and nitric acid in the mid infrared over a wide range of compositions and temperatures. It is shown that the main absorption features of both acids are determined by the activity of water and the ionic strength of the solution and that the spectra change continuously with composition and temperature. Hence it is possible to interpolate the absorption spectra from neighborhood spectra on a sufficiently narrow grid of compositions and temperatures.

In more detail, the following steps have been performed. First, a calibration procedure for the film thickness of the performed measurements based on the available room-temperature optical constants[3,4] allows the calculation of the imaginary part of the

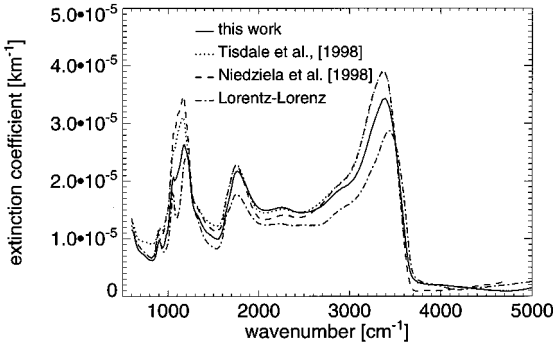

Figure 19. Comparison of sulfate aerosol extinction spectra (50 wt %, 220 K) based upon indexes of refraction of this work, Tisdale et al. and Niedziela et al. assuming a log-normal distribution of the aerosol at normal background conditions (see text). The fourth spectrum calculated on the basis of optical constants obtained by the Lorentz−Lorenz relationship clearly shows the unsuitability of this approximation for calculating the refractive indexes in the mid infrared.

refractive index, $k(\bar{\nu})$, for all binary spectra up to a concentration of 80 wt %. Based on the temperature-dependent absorption spectra obtained in this work, a parametrization of the temperature dependence of the extinction coefficient $\alpha(\bar{\nu})$ and the correlated imaginary refractive index k is introduced. A Kramers−Kronig analysis is used to calculate the real part of the refractive index, n, for spectra in the range of 183−293 K and 0−80 wt %.

Next, a mixing rule based on the Lorentz−Lorenz relationship is introduced, which allows the optical constants of ternary $H_2SO_4/HNO_3/H_2O$ solutions to be calculated in a wide range of atmospheric interest. The physical basis for the mixing rule is that in a ternary mixture the thermodynamic properties of the solution (ionic strengths, water acitivity) dominate the absorption characteristics, and that the mixing coefficients can be chosen such that the activity of water in a ternary solution is nearly equal to that of the binaries with corresponding concentrations. We show that the linear addition of absorption features of sulfate and nitrate are sufficiently precise to allow the composition of an unknown ternary solution to be determined by fitting the sum of the corresponding binary sulfuric and nitric acid spectra. The fit determines the composition to better than 1 wt %.

Finally, we tabulated values for $k(\bar{\nu})$ and $n(\bar{\nu})$ of selected compositions (5−10 wt % grid over the whole concentration and temperature range), from which spectra for all other concentrations and temperatures in the given range may be linearly interpolated. The data are available from the authors and from our Internet server (ftp ftp.mpch-mainz.mpg.de/pub/nwg for the uncompressed version or ftp ftp.mpch-mainz.mpg.de/pub/luo for the compressed version), together with the Fortran code to calculate the optical constants for the ternary solutions.

Acknowledgment. We thank Gerhard Schuster and Uwe Weers for experimental help. We are grateful to an anonymous referee for very careful reading of the manuscript. We would like to thank S. Massie and M. Hervig for advice and providing a useful computer routine which applies the Lorentz−Lorenz equation. Special thanks to Prof. Ludger Wöste and his group at the Free University of Berlin for the use of office and computer facilities. Support from the Friedrich-Ebert foundation (Grant for U.M.B.), the Bundesministerin für Bildung und Forschung (grant 01L09506), and the AFS Program (grant 07AF207/3) is gratefully acknowledged.

References and Notes

(1) Massie, S. T.; Thomas, G. E.; Mergenthaler, J. L.; Russell, J. M., III. *J. Geophys. Res.* **1996**, *101*, 23007−23019.
(2) Hervig, M. E.; Carslaw, K. S.; Peter, Th.; Biermann, U. M.; Gordley, L. L.; Redaelli, G.; Russell, J. M., III. *J. Geophys. Res.* **1997**, *102*, D23, 28185−28193.
(3) Palmer, K. F.; Williams, D. *Appl. Opt.* **1975**, *14*, 208−219.
(4) Querry, M. R.; Waring, R. C.; Holland, W. E.; Earls, L. M.; Herrman, M. D.; Nijm, W. P.; Hale, G. M. *J. Opt. Soc. Am.* **1974**, *64*, 39−46.
(5) Pinkley, L. W.; Williams, D. *J. Opt. Soc. Am.* **1976**, *66*, 122−124.
(6) Tisdale, R. T.; Glandorf, D. L.; Tolbert, M. A. *J. Geophys. Res.* **1998**, *103*, 25353−25370.
(7) Niedziela, R. F.; Norman, M. L.; Miller, R. E.; Worsnop, D. R. *Geophys. Res. Lett.* **1998**, *25*, 4477−4480.
(8) Niedziela, R. F.; Norman, M. L.; DeForest, C. L.; Miller, R. E.; Worsnop, D. R. *J. Phys. Chem. A* **1999**, *103* (40), 8030−8040.
(9) Querry, M. R.; Tyler, I. L. *J. Chem. Phys.* **1980**, *72*, 2495−2499.
(10) Boone, T. L.; Fuller, K. A.; Downing, H. D. *J. Phys. Chem.* **1980**, *84*, 2666−2667.
(11) Adams, R. W.; Dowing, H. D. *J. Opt. Soc. Am.* **1986**, *3(1)*, 22−28.
(12) Toon, O. B.; Tolbert, M. A.; Koehler, B. G.; Middlebrook, A. M.; Jordan, J. *J. Geophys. Res.* **1994**, 25631−25653.
(13) Berland, B. S.; Haynes, D. R.; Foster, K. L.; Tolbert, M. A.; George, S. M.; *J. Phys. Chem.* **1994**, *98*, 4358−4364.
(14) Middlebrook, A. M. Berland, B. S.; George, S. M.; Tolbert, M. A. *J. Geophys. Res.* **1994**, *99*, 25655−25666.
(15) Born, M.; Wolf, E. *Principle of Optics*; Pergamom Press: London, 1959.
(16) Hellwege, K. H.; Hellwege, A. M. *Landort-Börstein* **1962**, *II8*, 901.
(17) Haentzsch, A.; Dürigen, F. *Z. Phys. Chem.* **1928**, *136*, 1−17. **1928**, *134*, 413−452.
(18) Middlebrook, A. M.; Iraci, L. T.; McNeill, L. S.; Koehler, B. G.; Wilson, M. A.; Saastad, O. W.; Tolbert, M. A.; Hanson, D. R. *J. Geophys. Res.* **1998**, *98*, 20473−20481.
(19) Anthony, S. E.; Tisdale, R. T.; Disselkamp, R. S.; Tolbert, M. A.; Wilson, J. C. *Geophys. Res. Lett.* **1995**, *22*, 1105−1108.
(20) Luo, B. P.; Krieger, U. K.; Peter, Th. *Geophys. Res. Lett.* **1996**, *23*, 3707−3710.
(21) Gable, C. M.; Betz, H. F.; Maron, S. H. *J. Am. Chem. Soc.* **1950**, *72*, 1445−1448.
(22) Giguére, P. A.; Savoie, R. *Can. J. Chem.* **1960**, *38*, 2467−2476.
(23) Kopitzki, K. *Einführung in die Festkörperphysik*; Teubner/Studienbücher: Stuttgart, 1993.
(24) Wieliczka, D. M.; Weng, S.; Querry, M. R. *Appl. Opt.* **1989**, *28*, 1714−1719.
(25) Luo, B. P.; Carslaw, K. S.; Peter, Th.; Clegg, S. L. *Geophys. Res. Lett.* **1995**, *22*, 247−250.
(26) Anthony, S. E.; Onasch, T. B.; Tisdale, R. T.; Disselkamp, R. S.; Tolbert, M. A. *J. Geophys. Res.* **1997**, *102*, 10777−10784.
(27) Hofmann, D. J. *Nature* **1991**, *349*, 620.